

Joint Tx Power Allocation and Rx Power Splitting for SWIPT System with Multiple Nonlinear Energy Harvesting Circuits

Jae-Mo Kang, Il-Min Kim, *Senior Member, IEEE*, and Dong In Kim, *Senior Member, IEEE*

Abstract—We study the joint transmit (Tx) power allocation and receive (Rx) power splitting for simultaneous wireless information and power transfer (SWIPT). Considering the practical scenario of nonlinear energy harvesting (EH), we adopt the realistic nonlinear EH model for analysis. To address the critical nonlinearity issue due to the saturation, we propose to use multiple EH circuits in parallel. An important problem is to maximize the achievable rate by jointly optimizing Tx power allocation and Rx power splitting, which is a nonconvex problem. In this paper, we first derive the optimal solution for any number of EH circuits. Then we study how the number of EH circuits required to avoid the saturation should be determined. From the obtained results, we draw useful and interesting insights into the SWIPT system with nonlinear EH. Numerical results demonstrate that employing multiple EH circuits substantially enhances the SWIPT performance with nonlinear EH.

Index Terms—Multiple energy harvesting circuits, nonlinear energy harvesting, power allocation, power splitting, SWIPT.

I. INTRODUCTION

Simultaneous wireless information and power transfer (SWIPT) using radio frequency (RF) signals has been extensively studied in the literature [1]–[9]. In the most existing works on the SWIPT including [1]–[3], it was assumed that the amount of harvested energy linearly increases indefinitely with the input RF power of the energy harvesting (EH) circuit, namely, the *linear* EH model. However, this assumption is too idealistic because the linearity is valid only when the energy conversion efficiency is constant over the infinitely wide range of the input power level. As validated in many experimental results [10], [11], the practical EH circuit exhibits the nonlinear behavior because the energy conversion efficiency is different (not constant) depending on the input power level.

Very recently, to overcome the critical limitations of the linear EH model and to address the practicality issue of nonlinear EH, the SWIPT was studied for the realistic nonlinear EH models [4]–[9]. Among the various nonlinearity issues for EH, the most critical issue for the performance is the nonlinearity due to the saturation, because it severely limits the amount of harvested energy and the energy conversion efficiency of the EH circuit. Therefore, overcoming the nonlinearity due to the saturation is a practically very important issue in the SWIPT system. In the previous works on the nonlinear EH [4]–[9], various approaches have been developed to cope with the nonlinearity. However, none of these approaches were effective to overcome the saturation nonlinearity, because the

approaches were developed only with a single (nonlinear) EH circuit. Once the EH circuit saturates, there is no further performance improvement in the amount of harvested energy. An obvious, yet effective, way to overcome this limitation is to use multiple EH circuits in parallel. Then a very fundamental and important (but, non-trivial) question is: How to optimize the entire SWIPT system?; more specifically, how to jointly optimize the transmit (Tx) power and the receive (Rx) power splitting ratio? and how to determine the number of EH circuits that must be turned on? In the literature, this fundamental issue has not been studied. This motivated our work.

In this paper, we study the joint Tx power allocation and Rx power splitting for the SWIPT system with multiple nonlinear EH circuits. Adopting a realistic nonlinear EH model, we formulate the optimization problem to maximize the achievable rate with the harvested energy constraint and the average power constraint, which is nonconvex, and thus, challenging to solve. The contributions of this paper are as follows. First, for any number of EH circuits, we develop the jointly optimal Tx power allocation and Rx power splitting scheme. Second, we determine the required number of EH circuits to overcome the saturation nonlinearity. Also, from the obtained results, we draw various interesting and useful insights into the SWIPT system with nonlinear EH.

II. SYSTEM MODEL AND PROBLEM FORMULATION

We consider a point-to-point SWIPT system with one transmitter and one receiver, each equipped with a single antenna. Each block consists of N transmitted symbols: at the k th symbol period, the symbol is transmitted with power $P_k \geq 0$, where $k \in \{1, \dots, N\}$. The number N of symbols is assumed to be sufficiently large such that αN is an integer for arbitrary $0 < \alpha < 1$. Let h denote the power gain of the channel between the transmitter and the receiver, which is assumed to be quasi-static. Also, the channel state information (CSI) is assumed to be known at the transmitter and the receiver.¹

A. Linear and Nonlinear Energy Harvesting

In the previous works including [1]–[3], the linear EH model was adopted. In the linear EH model, the amount of harvested energy Q_L over the time duration of T is linearly proportional to the input power P_{in} of the EH circuit as follows:

$$Q_L = \zeta P_{in} T \quad (1)$$

where $0 < \zeta \leq 1$ is the energy conversion efficiency of the EH circuit, which is assumed to be a constant independent of

J.-M. Kang and I.-M. Kim are with the Department of Electrical and Computer Engineering, Queen's University, Kingston, ON K7L 3N6, Canada (e-mail: jaemo.kang@queensu.ca; ilmin.kim@queensu.ca).

D. I. Kim is with the School of Information and Communication Engineering, Sungkyunkwan University (SKKU), Suwon, 440-746, South Korea (e-mail: dikim@skku.ac.kr).

¹Recently, the received RF power based channel estimation scheme has been developed in [12], which can be used in our system to acquire the CSI at the transmitter and the receiver.

the input power. However, as validated in the experimental results [10], [11] and as analyzed in [6], the energy conversion efficiency of the actual EH circuit is different (not constant) over the different input power levels, meaning that the amount of harvested energy increases nonlinearly with the input power. Specifically, *only* when the input power is below a certain level, the energy conversion efficiency is not small (about 0.7 at the frequency of 915 MHz), and the amount of harvested energy increases almost linearly with the input power (e.g., see [7, Fig. 2], [9, Fig. 2]). On the other hand, when the input power exceeds a certain level, the energy conversion efficiency becomes very small (close to zero) due to the reverse breakdown, and the amount of harvested energy saturates.

In order to accurately model the nonlinear behavior of the practical EH circuit, several realistic nonlinear EH models have been suggested and studied in the recent literature [4]–[9]. Among the various nonlinear EH models, the nonlinear model used in [8], [9] is mathematically tractable and is shown to accurately match the experimental results [9, Fig. 2]. In this paper, for accuracy, practicality, and tractability of the analysis with useful insights, we adopt the nonlinear model of [8], [9]. In this nonlinear model, the amount of harvested energy is modeled based on the piecewise linear function as follows:

$$Q_{\text{NL}} = \begin{cases} \zeta P_{\text{in}} T, & \text{if } \zeta P_{\text{in}} \leq P_s \\ P_s T, & \text{if } \zeta P_{\text{in}} > P_s \end{cases} \quad (2)$$

where P_s ($\leq \zeta P_{\text{in}}$) denotes the maximum harvested power when the EH circuit is saturated.²

B. SWIPT with Multiple Nonlinear EH Circuits

In this paper, for analysis, we consider the dynamic power splitting architecture [1, Sec. III-A], which is the most general architecture for the SWIPT. At the receiver, the received power at the k th symbol period is dynamically split with a power splitting ratio $0 \leq \rho_k \leq 1$. At the transmitter, the transmit power P_k is dynamically adjusted under the average power constraint $\frac{1}{N} \sum_{k=1}^N P_k \leq P$, where P denotes a threshold for the average transmit power.

First, the $(1 - \rho_k)$ portion of the received power, i.e., $(1 - \rho_k)hP_k$, is used for information decoding (ID). The average achievable rate is given by

$$\mathcal{R}(\mathbf{P}, \boldsymbol{\rho}) = \frac{1}{N} \sum_{k=1}^N \mathbb{R}(P_k, \rho_k) = \frac{1}{N} \sum_{k \in \Omega} \mathbb{R}(P_k, \rho_k) \quad (3)$$

where \mathbf{P} and $\boldsymbol{\rho}$ are the vectors composed of P_k 's and ρ_k 's, respectively. Also, $\Omega = \{k : 0 \leq \rho_k < 1\}$ and

$$\mathbb{R}(x, y) = \log_2 \left(1 + \frac{(1-y)hx}{(1-y)\sigma_A^2 + \sigma_{\text{cov}}^2} \right). \quad (4)$$

In (4), σ_A^2 and σ_{cov}^2 are the variances of the antenna noise and the RF-to-baseband conversion noise, respectively.

Second, the remaining ρ_k portion of the received power is used for EH, and thus, the input power of the EH circuit is

² For a single diode rectifier, the maximum harvested power is given by $P_s = \frac{v_b^2}{4r_l}$, where v_b is the reverse breakdown voltage of the diode and r_l is the resistance of the load [10].

given by $P_{\text{in}} = \rho_k h P_k$. For the case of nonlinear EH, the amount of harvested energy as well as the energy conversion efficiency is strictly limited by the saturation effect, which is a critical issue for the performance of the SWIPT system. To address this issue, we propose to use multiple (nonlinear) EH circuits. Specifically, the input power is evenly split among M (≥ 1) EH circuits, such that no EH circuit enters the saturation region. Taking this approach and using the realistic nonlinear EH model of (2), the average net harvested energy can be written as

$$Q_{\text{NL}}(\mathbf{P}, \boldsymbol{\rho}) = \frac{1}{N} \left[\sum_{k \in \Omega^C} \sum_{i=1}^M Q_{\text{NL}} \left(P_k, \frac{1}{M} \right) + \sum_{k \in \Omega} \left(\sum_{i=1}^M Q_{\text{NL}} \left(P_k, \frac{\rho_k}{M} \right) - P_c T \right) \right] \quad (5)$$

where $\Omega^C = \{k : \rho_k = 1\}$ is the complement of the set Ω . Also, P_c ($< P_s$) denotes the circuit power consumed by the ID circuitry³ and

$$Q_{\text{NL}}(x, y) = \begin{cases} \zeta x y h T, & \text{if } \zeta x y h \leq P_s \\ P_s T, & \text{if } \zeta x y h > P_s \end{cases}. \quad (6)$$

C. Problem Formulation

In this paper, using the realistic nonlinear EH model, we aim to develop the jointly optimal Tx power allocation and Rx power splitting scheme for the SWIPT system with any number M of EH circuits, in the sense of maximizing the achievable rate under the constraints on the harvested energy and the average power. Thus, the problem is formulated as follows:

$$(P1) : \max_{\mathbf{P}, \boldsymbol{\rho}} \mathcal{R}(\mathbf{P}, \boldsymbol{\rho}) \quad (7)$$

$$\text{s.t. } Q_{\text{NL}}(\mathbf{P}, \boldsymbol{\rho}) \geq Q, \quad \frac{1}{N} \sum_{k=1}^N P_k \leq P \quad (8)$$

where Q is a threshold for the harvested energy. The problem (P1) is generally very challenging to solve due to the nonconvexity. To the best of our knowledge, in the literature, (P1) still remains unsolved even for the *linear* EH model,⁴ not to mention the *nonlinear* EH model.

III. JOINT TX POWER ALLOCATION AND RX POWER SPLITTING WITH MULTIPLE NONLINEAR EH CIRCUITS

A. Optimal Solution to (P1)

In this subsection, we derive the optimal solution to (P1) by converting it into a more tractable form. To this end, in the following, we first derive the optimal structure of the dynamic power splitting scheme.

³ Only the power consumption by ID circuitry is considered, because no power is consumed by the EH circuitry which consists of the passive devices such as the diode, inductor, and capacitor [1].

⁴ In [2, eq. (11)], an optimization problem similar to (P1) was studied for the linear EH model. However, in [2], the solution was derived only for a special case of $\rho_k \in \{0, 1\}$, $\forall k$, and $P_c = 0$, i.e., the time switching architecture [1, eq. (15)], with $M = 1$.

Lemma 1: The solution to (P1) takes the following form:

$$P_k = \begin{cases} P_{\text{EH}}, & k = 1, \dots, \alpha N \\ P_{\text{ID}}, & k = \alpha N + 1, \dots, N \end{cases}, \quad (9)$$

$$\rho_k = \begin{cases} 1, & k = 1, \dots, \alpha N \\ \rho, & k = \alpha N + 1, \dots, N \end{cases} \quad (10)$$

where $P_{\text{EH}} \geq 0$, $P_{\text{ID}} \geq 0$, $0 \leq \alpha \leq 1$, and $0 \leq \rho < 1$ are the variables to be determined.

Proof: See Appendix A. ■

Lemma 1 means that only the EH (no ID) has to be carried out during the α portion of the block, and both EH and ID has to be carried out during the remaining $(1 - \alpha)$ portion of the block. The result of Lemma 1 is very interesting and practically useful, because it indicates that the jointly optimal Tx power allocation and Rx power splitting scheme reduces to the on-off power splitting architecture [1, eq. (17)], which is much simpler than the dynamic power splitting architecture. Furthermore, it is very important to note that using Lemma 1, the original optimization of (P1) over the two N -dimensional vectors \mathbf{P} and $\boldsymbol{\rho}$ can be substantially simplified to the optimization only over the four scalars P_{EH} , P_{ID} , ρ , and α , as follows:

$$(P1') : \quad \max_{P_{\text{EH}}, P_{\text{ID}}, \alpha, \rho} (1 - \alpha) \mathbb{R}(P_{\text{ID}}, \rho) \quad (11)$$

$$\text{s.t.} \quad \alpha M \mathbb{Q}_{\text{NL}} \left(P_{\text{EH}}, \frac{1}{M} \right) + (1 - \alpha) M \mathbb{Q}_{\text{NL}} \left(P_{\text{ID}}, \frac{\rho}{M} \right) - (1 - \alpha) P_c T \geq Q, \quad (12)$$

$$\alpha P_{\text{EH}} + (1 - \alpha) P_{\text{ID}} \leq P \quad (13)$$

Note that by Lemma 1, it possible to significantly reduce the complexity to solve (P1). However, the converted problem (P1') is still nonconvex because the variables are coupled. In this paper, by determining the variables P_{EH} , P_{ID} , and ρ in terms of α , we can obtain the optimal solution to (P1') very efficiently, as shown in the following.

Theorem 1: The solution to (P1') is given by

$$\alpha^* = \arg \max_{\alpha_{\text{low}} \leq \alpha \leq 1} (1 - \alpha) \mathbb{R}(P_{\text{ID}}(\alpha), \rho(\alpha)), \quad (14)$$

$$\rho^*(\alpha^*) = \min \{ \rho_1(\alpha^*), \rho_2(\alpha^*) \}, \quad (15)$$

$$P_{\text{EH}}^*(\alpha^*) = \begin{cases} \frac{Q + (1 - \alpha^*) P_c T - \zeta \rho^*(\alpha^*) h P T}{\alpha^* \zeta (1 - \rho^*(\alpha^*)) h T}, & \text{if } \alpha^* > 0 \\ 0, & \text{if } \alpha^* = 0 \end{cases}, \quad (16)$$

$$P_{\text{ID}}^*(\alpha^*) = \begin{cases} \frac{\zeta h P T - Q - (1 - \alpha^*) P_c T}{(1 - \alpha^*) \zeta (1 - \rho^*(\alpha^*)) h T}, & \text{if } \alpha^* < 1 \\ 0, & \text{if } \alpha^* = 1 \end{cases}. \quad (17)$$

In (14), $\alpha_{\text{low}} = \max \left\{ 1 - \frac{\zeta h P T - Q}{P_c T}, 0 \right\}$. Also, $\rho(\alpha)$ and $P_{\text{ID}}(\alpha)$ are defined similarly as in (14) and (17), respectively. In (14), the value of α^* can be determined by the one-dimensional searching. In (15), $\rho_1(\alpha) = \frac{Q + (1 - \alpha) P_c T}{\zeta h P T}$ and $\rho_2(\alpha) = \frac{(1 - \alpha) M P_s T}{(1 - \alpha) M P_s T + \zeta h P T - Q - (1 - \alpha) P_c T}$.

Proof: See Appendix B. ■

Substituting (14)–(17) into (9) and (10), the optimal solution to (P1) can be obtained. The result of Theorem 1 is very useful in practice due to its very low complexity. From Theorem 1, one can also obtain the insights as follows: As

α^* decreases (except $\alpha^* = 0$), the power $P_{\text{EH}}^*(\alpha^*)$ used only for EH increases to meet the harvested energy constraint. The remaining power $P_{\text{ID}}^*(\alpha^*)$ is used for both EH and ID, and thus, it decreases as α^* decreases.

B. Determining the Number of EH Circuits

In the previous subsection, we derived the optimal solution to (P1) for any given number M (≥ 1) of EH circuits. In this subsection, we determine the number of EH circuits required to overcome the saturation nonlinearity. The fundamental idea is as follows: The number M of EH circuits increases one by one until none of the EH circuits operate in the saturation region. Specifically, initially setting $M = 1$, the value of M increases to $M + 1$ if the (effective) input power $P_{\text{in}}^M = \max \{ h P_{\text{EH}}^*(\alpha^*), h P_{\text{ID}}^*(\alpha^*) \} - \frac{(M-1)P_s}{\zeta}$ fed into the M th circuit exceeds the saturation threshold $\frac{P_s}{\zeta}$. This proceeds until M reaches M_{max} , where M_{max} is the maximum number of EH circuits. The proposed algorithm is presented in Algorithm 1.

Algorithm 1 Proposed algorithm for determining the number of EH circuits

-
- 1: Set $M = 1$.
 - 2: **while** $M > M_{\text{max}}$ **do**
 - 3: Compute $P_{\text{EH}}^*(\alpha^*)$ and $P_{\text{ID}}^*(\alpha^*)$ according to (16) and (17), respectively.
 - 4: Compute $P_{\text{in}}^M = \max \{ h P_{\text{EH}}^*(\alpha^*), h P_{\text{ID}}^*(\alpha^*) \} - \frac{(M-1)P_s}{\zeta}$.
 - 5: **if** $P_{\text{in}}^M > \frac{P_s}{\zeta}$ **then**
 - 6: Set $M \leftarrow M + 1$.
 - 7: **end if**
 - 8: **end while**
-

IV. NUMERICAL RESULTS

In this section, we compare the performance of the proposed and existing schemes. For the comparison purpose, we extend the existing Tx power allocation and Rx *time switching* scheme of [2] developed for a single linear EH circuit model, to the adopted model of multiple nonlinear EH circuits, which can be obtained as a special case of Theorem 1 with $\rho = 0$ (i.e., the solution to (P1') when $\rho = 0$). In the numerical simulations, we consider the Rician fading model: $g = \sqrt{\frac{r}{r+1}} g_{\text{LOS}} + \sqrt{\frac{1}{r+1}} g_{\text{scatter}}$, where g is the fading channel such that $h = |g|^2$; g_{LOS} the line-of-sight (LOS) component; g_{scatter} the scattering component following the Gaussian distribution with zero-mean and variance $\sigma_{\text{scatter}}^2$; and r the Rician factor. We set $r = 2$ and $|g_{\text{LOS}}|^2 = \sigma_{\text{scatter}}^2 = -30$ dBW. Also, we set $T = 1$ s, $\zeta = 1$, $P_s = 0.4hP$, $P_c = 0.3P_s$, $M_{\text{max}} = \left\lceil \frac{\zeta h P}{P_s} \right\rceil$, and $\sigma_A^2 = \sigma_{\text{cov}}^2 = \sigma^2$, where $\bar{h} = \frac{r}{r+1} |g_{\text{LOS}}|^2 + \frac{1}{r+1} \sigma_{\text{scatter}}^2$ is the average channel power gain and $\lceil x \rceil$ is the smallest integer not less than x . The value of σ^2 is chosen such that $\frac{\bar{h} P}{\sigma^2} = 20$ dB. The results are averaged over 10^4 different channel realizations.

In Fig. 1, the rate-energy (R-E) tradeoffs of the proposed and existing schemes are shown for $M = M^*$ when $P \in \{1.5, 3\}$ W and for $P = 2$ W when $M = \{1, M^*\}$, where M^* denotes the number of EH circuits obtained by Algorithm 1.

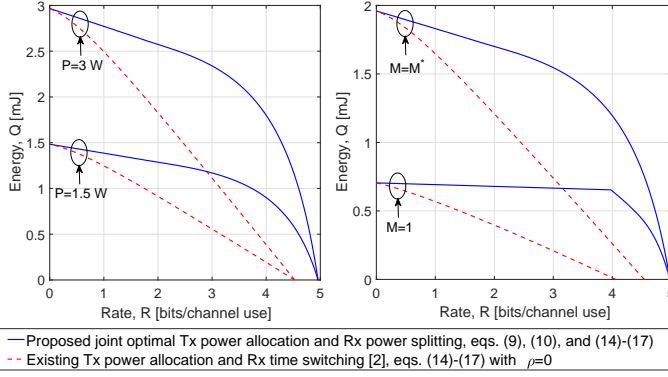


Fig. 1. R-E tradeoffs of the proposed and existing schemes for $M = M^*$ when $P \in \{1.5, 3\}$ W and for $P = 2$ W when $M = \{1, M^*\}$.

Also, the R-E region is defined as $\mathcal{C}_{\text{NL}}^M = \bigcup_{\mathbf{P}, \rho} \{(R, Q) : R \leq \mathcal{R}(\mathbf{P}, \rho), Q \leq \mathcal{Q}_{\text{NL}}(\mathbf{P}, \rho)\}$, which contains all possible pairs of the rate and harvested energy with M EH nonlinear circuits. From Fig. 1, it can be seen that the proposed joint Tx power allocation and Rx power splitting scheme considerably outperforms the existing Tx power allocation and Rx time switching scheme. Also, it can be observed that by adaptively determining the number of EH circuits, the R-E tradeoff performance with nonlinear EH is substantially improved. This clearly shows the benefit and effectiveness of using multiple EH circuits for the practical SWIPT system.

V. CONCLUSION

We studied the joint Tx power allocation and Rx power splitting for the SWIPT system with nonlinear EH. We proposed to use multiple EH circuits to overcome the saturation nonlinearity. Using the realistic nonlinear EH model, we developed the jointly optimal Tx power allocation and Rx power splitting scheme. Also, we developed the algorithm to determine the number of EH circuits. The obtained results gave us the useful and interesting insights. The numerical results showed that the SWIPT performance considerably improves when multiple EH circuits are used.

APPENDIX A: PROOF OF LEMMA 1

The optimal objective value of (P1) depends only on the cardinality of the set Ω . Also, in (P1), it must be $|\Omega^C| = N - |\Omega| = \alpha N$ for some $0 \leq \alpha \leq 1$ since the amount of circuit power consumption reduces from P_c to $(1 - \alpha)P_c$. Thus, without loss of any optimality, we can take $\Omega = \{\alpha N + 1, \dots, N\}$ and $\rho_k = 1$, $k \in \Omega^C = \{1, \dots, \alpha N\}$. Consequently, given α and ρ , the optimization of (P1) becomes convex in \mathbf{P} . From the Karush-Kuhn-Tucker conditions, we have $P^*(\alpha, \rho_k) = \frac{1}{\nu - \mu \zeta \rho_k h} - \frac{1}{h} \left(\sigma_A^2 + \frac{\sigma_{\text{cov}}^2}{1 - \rho_k} \right)$, $k = \alpha N + 1, \dots, N$, where $\mu \geq 0$ and $\nu \geq 0$ are the Lagrange multipliers associated with the constraints of (8) satisfying $\mu - \nu \zeta h \geq \frac{h}{\sigma_A^2 + \sigma_{\text{cov}}^2}$. Given α , both $\mathbb{R}(P^*(\alpha, \rho_k), \rho_k)$ and $\mathcal{Q}_{\text{NL}}(P^*(\alpha, \rho_k), \frac{\rho_k}{M})$ are concave in ρ_k , $k = \alpha N + 1, \dots, N$. Therefore, we have $\frac{1}{N} \sum_{k=\alpha N+1}^N C(P^*(\alpha, \rho_k), \rho_k) \leq (1 - \alpha)C(P^*(\alpha, \rho), \rho)$ and $\frac{1}{N} \sum_{k=\alpha N+1}^N E_{\text{NL}}(P^*(\alpha, \rho_k), \frac{\rho_k}{M}) \leq$

$(1 - \alpha)E_{\text{NL}}(P^*(\alpha, \rho), \frac{\rho}{M})$, where $\rho = \frac{1}{(1 - \alpha)N} \sum_{k=\alpha N+1}^N \rho_k$. From this, with given α , the solution to (P1) can be written as in (9) and (10), where $P_{\text{EH}} = \frac{1}{N} \sum_{k=1}^{\alpha N} P_k$ and $P_{\text{ID}} = P^*(\alpha, \rho)$, $k = \alpha N + 1, \dots, N$.

APPENDIX B: PROOF OF THEOREM 1

In (P1'), both the constraints of (8) must be satisfied with equalities. Thus, the constraint of (8) can be divided into the following five constraints: (8a): $Q_{\text{EH}} + Q_{\text{ID}} - (1 - \alpha)P_c T = Q$; (8b): $\alpha \zeta h P_{\text{EH}} T \geq Q_{\text{EH}}$; (8c): $(1 - \alpha) \zeta \rho h P_{\text{ID}} T \geq Q_{\text{ID}}$; (8d): $\zeta h P_{\text{EH}} \leq M P_s T$; and (8e): $\zeta \rho h P_{\text{ID}} \leq M P_s T$. If $\alpha = 0$, we have $P_{\text{EH}} = 0$, $P_{\text{ID}} = P$, and $\rho = \frac{Q}{\zeta h P T}$. If $\alpha = 1$, we can set $P_{\text{ID}} = 0$. If $0 < \alpha < 1$, from (8b) and (8c), we have $P_{\text{EH}} = \frac{Q_{\text{EH}}}{\alpha \zeta h T}$ and $P_{\text{ID}} = \frac{Q_{\text{ID}}}{(1 - \alpha) \zeta \rho h T}$, respectively. Thus, from (8a), we obtain $Q_{\text{EH}} = \frac{1}{1 - \rho} (Q + (1 - \alpha)P_c T - \zeta \rho h P T)$ and $Q_{\text{ID}} = \frac{\zeta \rho h}{1 - \rho} (P T - Q - (1 - \alpha)P_c T)$, respectively. Substituting these Q_{EH} and Q_{ID} into P_{EH} and P_{ID} , respectively, we can obtain $P_{\text{EH}}(\alpha)$ and $P_{\text{ID}}(\alpha)$ similarly as in (16) and (17), respectively. To satisfy (8d), it must be $\rho \geq \max \left\{ \frac{Q + (1 - \alpha)P_c T - \alpha M P_s T}{\zeta h P T - \alpha M P_s T}, 0 \right\}$. Also, to satisfy both (8e) and $P_{\text{EH}}(\alpha) \geq 0$, it must be $\rho \leq \min \{\rho_1(\alpha), \rho_2(\alpha)\}$. To ensure $\rho_1(\alpha) \leq 1$, $\rho_2(\alpha) \leq 1$, and $P_{\text{ID}}(\alpha) \geq 0$, it must be $\alpha_{\text{low}} \leq \alpha \leq 1$. Since the objective function is increasing in ρ when $P_{\text{ID}}(\alpha)$ is substituted, the optimal ρ is given by $\rho(\alpha) = \min \{\rho_1(\alpha), \rho_2(\alpha)\}$. Then the optimal α can be determined by maximizing $(1 - \alpha)\mathbb{R}(P_{\text{ID}}(\alpha), \rho(\alpha))$ over $\alpha_{\text{low}} \leq \alpha \leq 1$.

REFERENCES

- [1] X. Zhou, R. Zhang, and C. K. Ho, "Wireless information and power transfer: Architecture design and rate-energy tradeoff," *IEEE Trans. Commun.*, vol. 61, no. 11, pp. 4753–4767, Nov. 2013.
- [2] R. Zhang and C. K. Ho, "MIMO broadcasting for simultaneous wireless information and power transfer," *IEEE Trans. Wireless Commun.*, vol. 12, no. 5, pp. 1989–2001, May. 2013.
- [3] I.-M. Kim and D. I. Kim, "Wireless information and power transfer: Rate-energy tradeoff for equi-probable arbitrary-shaped discrete inputs," *IEEE Trans. Wireless Commun.*, vol. 15, no. 6, pp. 4393–4407, Jun. 2016.
- [4] J.-M. Kang, I.-M. Kim, and D. I. Kim, "Wireless information and power transfer: Rate-energy tradeoff for nonlinear energy harvesting," *IEEE Trans. Wireless Commun.*, vol. 17, no. 3, pp. 1966–1981, Mar. 2018.
- [5] J.-M. Kang, I.-M. Kim, and D. I. Kim, "Mode switching for SWIPT over fading channel with nonlinear energy harvesting," *IEEE Wireless Commun. Lett.*, vol. 6, no. 5, pp. 678–660, Oct. 2017.
- [6] B. Clerckx and E. Bayguzina, "Waveform design for wireless power transfer," *IEEE Trans. Signal Process.*, vol. 64, no. 23, pp. 6313–6328, Dec. 2016.
- [7] E. Boshkovska *et al.*, "Practical nonlinear energy harvesting model and resource allocation for SWIPT systems," *IEEE Commun. Lett.*, vol. 19, no. 12, pp. 2082–2085, Dec. 2015.
- [8] Y. J. Dong *et al.*, "Performance of wireless powered amplify and forward relaying over Nakagami-m fading channels with nonlinear energy harvester," *IEEE Commun. Lett.*, vol. 20, no. 4, pp. 672–675, Apr. 2016.
- [9] L. Shi *et al.*, "Profit maximization in wireless powered communications with improved non-linear energy conversion and storage efficiencies," in *Proc. IEEE ICC*, 2017, pp. 1–6.
- [10] C. Valenta and G. Durgin, "Harvesting wireless power: Survey of energy harvester conversion efficiency in far-field wireless power transfer systems," *IEEE Microw. Mag.*, vol. 15, no. 4, pp. 108–120, Jun. 2014.
- [11] J. Guo and X. Zhu, "An improved analytical model for RF-DC conversion efficiency in microwave rectifiers," in *Proc. IEEE MTT-S Int. Microw. Symp. Dig.*, 2012, pp. 1–3.
- [12] K. W. Choi *et al.*, "Received power-based channel estimation for energy beamforming in multiple-antenna RF energy transfer system," *IEEE Trans. Signal Process.*, vol. 65, no. 6, pp. 1461–1476, Mar. 2017.